International Journal of Innovative
Computing, Information and Control
Volume **8**, Number **3(A)**, March **2012**

ICIC International ©2012 ISSN 1349-4198
pp. **1611–1634**

ROBUST COMPENSATOR SYNTHESIS FOR ANTIWINDUP DESIGN WITH COPRIME FACTOR UNCERTAINTIES

Jieh-Shian Young

Institute of Vehicle Engineering
National Changhua University of Education
No. 1, Jin-De Road, Chang-hua 500, Taiwan
jsyoung@cc.ncue.edu.tw

Received December 2010; revised April 2011

Abstract. *This paper studies the antiwindup synthesis problems for plants with coprime factor uncertainties. The proposed technique utilizes an equivalent framework of compensated systems to investigate the robustness of the antiwindup compensators. The penalty operators of the input saturation are studied originally in general cases. Robustness criteria are proposed for an antiwindup compensated system with different model uncertainties including the additive uncertainty and the coprime factor uncertainties. Linear matrix inequality based techniques can synthesize an antiwindup compensator to conform the system to better robustness requirements for input saturation problems. The simulation results show that the antiwindup compensator synthesized in this paper is more adequate to plants with coprime factor uncertainties. A system which is a rotorcraft model in hover flight condition is presented as a practical example to show the robustness and the performance of the antiwindup compensator from the proposed approach.*
Keywords: Antiwindup, Coprime factor uncertainty, Input saturation, Linear matrix inequality (LMI), Robustness

1. **Introduction.** Researchers have paid significant attention to antiwindup synthesis for linear control systems over last two decades. An antiwindup compensator is intended to recover as much as possible performance for a compensated system in the presence of input saturation. Early studies on this topic developed many qualitative approaches to particular instances of antiwindup synthesis (e.g., [1-3]). Campo et al. constructed an antiwindup augmentation configuration [4]. That is perhaps the most typical embodiment configuration. The antiwindup technique has become one of the most popular solutions to input saturation problems. More recent studies presented a number of antiwindup schemes with better stability and performance. These studies proposed many systematic approaches, including the H^∞ based optimal control technique [5-7], the reference governor scheme [8-10] and the linear matrix inequality (LMI) based techniques (see e.g., [11-13]). The antiwindup synthesis is still supported by further theoretical studies and applications. For more comprehensive overviews of antiwindup approaches, see the work in [14]. Instead of going into detail on the above approaches, this paper focuses on antiwindup synthesis to ensure the robustness of the compensated system in the presence of model uncertainties.

Robust controller design has been a prominent issue in control research for many years. For instance, Sun et al. proposed an approach to the synthesis for a nonlinear robust controller and a parameter updating law simultaneously by using modified adaptive backstepping sliding mode control and Lyapunov methods [15]. Some of the robust nonlinear control syntheses were presented based on the LMI approach [16,17]. The model uncertainty and input saturation control problems are usually separated in syntheses. Gomes

da Silva and Tarbouriech proposed an approach to an antiwindup gain for larger regions of stability in linear systems [18]. Hu et al. also presented LMI-based synthesis methods for the optimization of the regional stability and performance of linear antiwindup compensators [12]. The static antiwindup problem for plants with magnitude and rate saturation was addressed by Galeani et al. [19]. They also provided an LMI-based procedure for the construction of a linear antiwindup gain by using the generalized sector condition. The input saturation in their approach can be regarded as another type of uncertainty that can be handled by the standard robust control techniques [20]. Turner et al. accounted for the model uncertainty in synthesis [21]. Based on [21], they treated the robustness problem of antiwindup synthesis with additive model uncertainty [22]. They also discussed the requirements of the stability robustness optimization and proposed the LMI approach to optimize the robustness and performance of antiwindup synthesis. The coprime factor uncertainties were studied in [23]. Essentially, for the sake of small gain theorem, the coprime factor uncertainties can release the constraint of the same pole number on the closed right half plane (RHP) for all possible plants within uncertainties. Deng et al. proposed a design scheme for the output tracking of nonlinear feedback systems with perturbation based on robust right coprime factorization [24]. Young synthesized the decoupling controller for non-minimum phase plants with different pole numbers on RHP within uncertainties [25].

The purpose of this paper is to obtain the robustness requirements of antiwindup synthesis for plants subject to coprime factor uncertainties and input saturation. Inspired by [22], this paper constructs an equivalent framework of the compensated systems to facilitate the construction of uncertainty I/O maps. Analysis of the coprime factor uncertainties in antiwindup synthesis can be achieved by using this equivalent framework. The stability robustness requirements addressed in this paper can be also represented by an LMI. They cannot be extended straightforward from those in [22] due to significantly different equivalent frameworks and penalty operators. Conversely, the results are more generally compared with those in [22]. This paper originally studies the penalty matrix operators and the robustness criteria of an antiwindup compensator for a plant subject to model uncertainties such as the additive uncertainty and the coprime factor uncertainties. Without loss of generality, this study considers the left coprime factor uncertainties of plants. Finally, the simulation results compared with those in [22] show that the proposed approach is more appropriate to plants with coprime factor uncertainties in both time responses and frequency responses.

This paper uses standard notations. RH_∞ denotes the space of proper, real-rational functions with no poses on the closed RHP, $\|G(s)\|_\infty$ denotes the H_∞-norm of $G(s) \in RH_\infty$, and a matrix $P > 0$ ($P < 0$) means P is a positive (negative) definite matrix. In particular, $\underline{\underline{SC}}$ denotes the Schur complement operation for a negative definite matrix, $\underset{X_1,\cdots,X_n}{\underline{\underline{CT}}}$ denotes the operation of the congruence transformation $diag\,(X_1, \cdots, X_n)$, and $\overset{S}{=}$ denotes the state space representation of a transfer function, i.e., $G(s) \overset{S}{=} \left[\begin{array}{c|c} A & B \\ \hline C & D \end{array}\right]$ means $G(s) = C(sI - A)^{-1}B + D$. An induced L_2-norm of an operator Γ is defined as $\|\Gamma\|_{i,2} = \sup_{x\neq 0, x\in L_2} \frac{\|\Gamma x\|_2}{\|x\|_2}$, where $\|x\|_2$ is the L_2-norm of a vector $x(t)$. $\|\Gamma\|_{i,2} = \|\Gamma\|_\infty$ if Γ is a linear operator. Hereafter in this study, a transfer function G may be written instead of $G(s)$, effectively implying the s-dependence of the transfer function matrix.

2. The Antiwindup Framework with Coprime Factor Uncertainties.

Consider the configuration of linear systems in Figure 1, where G_2 is the nominal plant of the

true plant, $\tilde{G}_2$. $G_2 = M^{-1}N = \tilde{N}\tilde{M}^{-1}$ is a $p \times q$ multiinput-multioutput (MIMO) controlled plant, where (M, N) and $(\tilde{M}, \tilde{N})$ are the left and right coprime factor pairs of G_2, respectively. $\tilde{G}_2 = (M + W\tilde{\Delta}_M W_M)^{-1}(N + W\tilde{\Delta}_N W_N)$ represents a plant subject to the frequency-weighted coprime factor uncertainties where W, W_N and W_M, are all known. Without loss of generality, let the coprime factor uncertainties, Δ_N and Δ_M, be frequency-weighted inherently, i.e., $\Delta_N = W\tilde{\Delta}_N W_N$ and $\Delta_M = W\tilde{\Delta}_M W_M$. Thus, $\tilde{G}_2 = (I + M^{-1}\Delta_M)^{-1}(G_2 + M^{-1}\Delta_N)$.

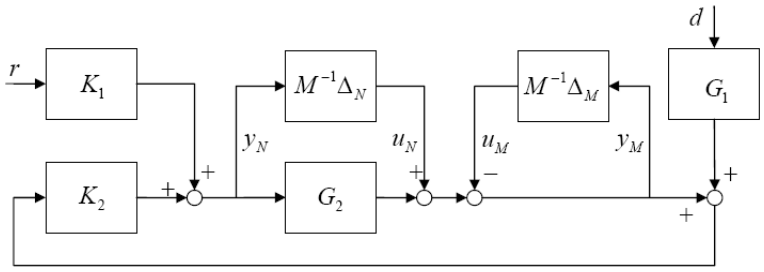

FIGURE 1. The robust control problems with coprime factor uncertainties

In this paper, the robust bound evaluated for the compensated system is $\| (-M^{-1}\Delta_M, M^{-1}\Delta_N) \|_\infty$ instead of $\|(-\Delta_M, \Delta_N)\|_\infty$ since $\|(-M^{-1}\Delta_M, M^{-1}\Delta_N)\|_\infty$ retains the bound of uncertainties for different possible denominators of the left coprime factors, M. Figure 1 shows that the I/O maps between the coprime factor uncertainties are

$$\begin{pmatrix} y_M \\ y_N \end{pmatrix} = \begin{pmatrix} -(I - G_2K_2)^{-1} & (I - G_2K_2)^{-1} \\ -K_2(I - G_2K_2)^{-1} & K_2(I - G_2K_2)^{-1} \end{pmatrix} \begin{pmatrix} u_M \\ u_N \end{pmatrix}$$

According to the small gain theory, if and only if the compensated system is stable, then

$$\left\| \begin{pmatrix} -(I - G_2K_2)^{-1} & (I - G_2K_2)^{-1} \\ -K_2(I - G_2K_2)^{-1} & K_2(I - G_2K_2)^{-1} \end{pmatrix} \begin{pmatrix} M^{-1}\Delta_M & 0 \\ 0 & M^{-1}\Delta_N \end{pmatrix} \right\|_\infty < 1,$$

or

$$\left\| \begin{pmatrix} I \\ K_2 \end{pmatrix} (I - G_2K_2)^{-1} \begin{pmatrix} -M^{-1}\Delta_M & M^{-1}\Delta_N \end{pmatrix} \right\|_\infty < 1. \tag{1}$$

If $M^{-1}\Delta_M = 0$, the system depicted in Figure 1 will degenerate into a plant subject to additive uncertainties, i.e., $\|K_2(I - G_2K_2)^{-1}M^{-1}\Delta_N\|_\infty < 1$. In case G_2 has a stabilizable and detectable state space representation as

$$G_2 \stackrel{s}{=} \left[\begin{array}{c|c} A & B \\ \hline C & D \end{array}\right], \tag{2}$$

the state space representation of its right coprime factors can be

$$\begin{pmatrix} \tilde{M} \\ \tilde{N} \end{pmatrix} \stackrel{s}{=} \left[\begin{array}{c|c} A + BF & B \\ \hline F & I \\ C + DF & D \end{array}\right], \tag{3}$$

where the eigenvalues of $A + BF$ are all on open left half plane (LHP).

Figure 2 shows a typical antiwindup synthesis for a plant subject to coprime factor uncertainties. The system will be a problem of the antiwindup synthesis if $M^{-1}\Delta_N = 0$ and $M^{-1}\Delta_M = 0$. In addition, it will become an internal model control (IMC) antiwindup scheme if $\hat{M}$ is equal to unity. Based on the suggestion of Weston and Postlethwaite, this paper states that $\hat{M}$ is equal to the right coprime denominator factor of G_2, or $\hat{M} = \tilde{M}$ (refer to [26] for the details). The aim of the antiwindup design is to synthesize $\hat{M} - I$ and $G_2\hat{M}$ blocks in Figure 2. Inherently, the feedback controller, K_2, should robustly stabilize

the plant if there is no input saturation. Therefore, we make the following assumptions throughout this paper.

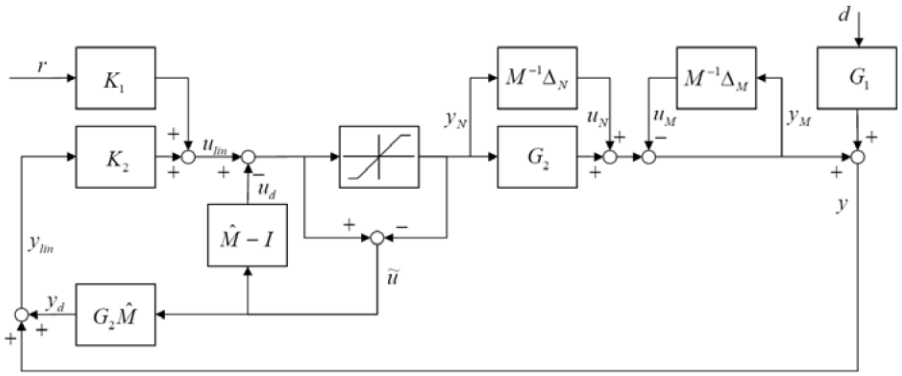

FIGURE 2. Antiwindup synthesis with coprime factor uncertainties

Assumption 1. $G_1 \in RH_\infty$;
Assumption 2. $\begin{pmatrix} \Delta_M & \Delta_N \end{pmatrix} \in RH_\infty$;
Assumption 3. $\begin{pmatrix} I & -K_2 \\ -\tilde{G}_2 & I \end{pmatrix}^{-1} \in RH_\infty \quad \forall \begin{pmatrix} \Delta_M & \Delta_N \end{pmatrix} \in RH_\infty$.

In Assumption 1, the system will maintain global finite-gain stability in case of input saturation. Assumption 2 is necessary for the small-gain theory even though the poles of $(M+\Delta_M)^{-1}$ may not be always on open LHP, i.e., the uncertain plant $\tilde{G}_2$ is not always stable within uncertainties. Assumption 3 indicates that the linear closed-loop system is robustly asymptotically stable and well-posed within uncertainties. That is, the system compensated by K_2 is robustly asymptotically stable in the presence of coprime factor uncertainties without input saturation nonlinearity. By this assumption and according to (1), $\left\| \begin{pmatrix} -M^{-1}\Delta_M & M^{-1}\Delta_N \end{pmatrix} \right\|_\infty < \dfrac{1}{\delta}$, where

$$\left\| \begin{pmatrix} I \\ K_2 \end{pmatrix} (I - G_2K_2)^{-1} \right\|_\infty = \delta. \tag{4}$$

3. **Penalty Operator of Input Saturation for Antiwindup Synthesis.** Figure 3 shows the equivalent representation of Figure 2 with $\hat{M} = \tilde{M}$, where $\Gamma(u_{lin})$ is the mapping from u_{lin} to $\tilde{u}$. All signals are the same as those in Figure 2. Figure 4 shows the equivalent block diagram of $\Gamma(u_{lin})$, where Σ is a nonlinear operator substituting the dead zone block diagram in Figure 3 and it can be a diagonal matrix, i.e.,

$$\Sigma = \begin{pmatrix} \sigma_1 & & & 0 \\ & \sigma_2 & & \\ & & \ddots & \\ 0 & & & \sigma_q \end{pmatrix}$$

and $\sigma_i \in [0,1)$, $i = 1, 2, \cdots, q$. $I + (\tilde{M} - I)\Sigma$ is invertible for all possible values of Σ, i.e., the nonlinear mapping from u_{lin} to $\tilde{u}$ can be expressed as $\tilde{u} = \Gamma(u_{lin}) = \Sigma \left[I + (\tilde{M} - I)\Sigma \right]^{-1} u_{lin}$.

Let $\tilde{u} \equiv \Gamma_\Sigma u_{lin}$, then

$$\Gamma_\Sigma = \Sigma \left[I + (\tilde{M} - I)\Sigma \right]^{-1}, \tag{5}$$

where Γ_Σ is also a nonlinear operator since Σ is a nonlinear operator. According to (5), the I/O maps between the coprime factor uncertainties in Figure 3 become

$$\begin{pmatrix} y_M \\ y_N \end{pmatrix} = \begin{pmatrix} -(I-G_2K_2)^{-1} + \tilde{N}\Gamma_\Sigma K_2(I-G_2K_2)^{-1} & (I-G_2K_2)^{-1} - \tilde{N}\Gamma_\Sigma K_2(I-G_2K_2)^{-1} \\ -(I-\hat{M}\Gamma_\Sigma)K_2(I-G_2K_2)^{-1} & (I-\hat{M}\Gamma_\Sigma)K_2(I-G_2K_2)^{-1} \end{pmatrix} \begin{pmatrix} u_M \\ u_N \end{pmatrix}$$
$$= \begin{pmatrix} I & -\tilde{N}\Gamma_\Sigma \\ 0 & I-\hat{M}\Gamma_\Sigma \end{pmatrix} \begin{pmatrix} -(I-G_2K_2)^{-1} & (I-G_2K_2)^{-1} \\ -K_2(I-G_2K_2)^{-1} & K_2(I-G_2K_2)^{-1} \end{pmatrix} \begin{pmatrix} u_M \\ u_N \end{pmatrix}.$$

According to the small gain theory,

$$\left\| \begin{pmatrix} I & -\tilde{N}\Gamma_\Sigma \\ 0 & I-\tilde{M}\Gamma_\Sigma \end{pmatrix} \begin{pmatrix} -(I-G_2K_2)^{-1} & (I-G_2K_2)^{-1} \\ -K_2(I-G_2K_2)^{-1} & K_2(I-G_2K_2)^{-1} \end{pmatrix} \begin{pmatrix} M^{-1}\Delta_M & 0 \\ 0 & M^{-1}\Delta_N \end{pmatrix} \right\|_{i,2} < 1,$$

or

$$\left\| \begin{pmatrix} I & -\tilde{N}\Gamma_\Sigma \\ 0 & I-\tilde{M}\Gamma_\Sigma \end{pmatrix} \begin{pmatrix} I \\ K_2 \end{pmatrix} (I-G_2K_2)^{-1} \begin{pmatrix} -M^{-1}\Delta_M & M^{-1}\Delta_N \end{pmatrix} \right\|_{i,2} < 1. \quad (6)$$

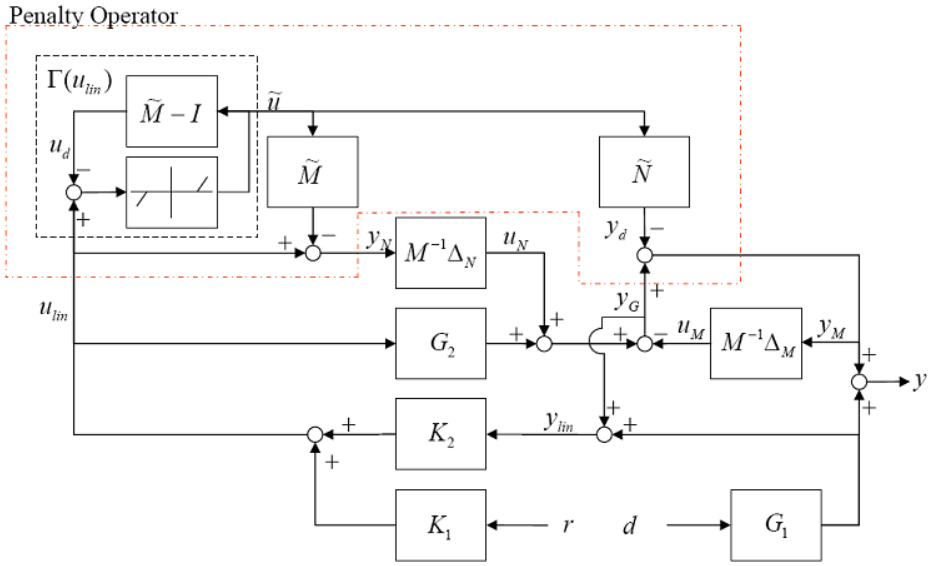

FIGURE 3. Equivalent representation of Figure 2 with $\hat{M} = \tilde{M}$

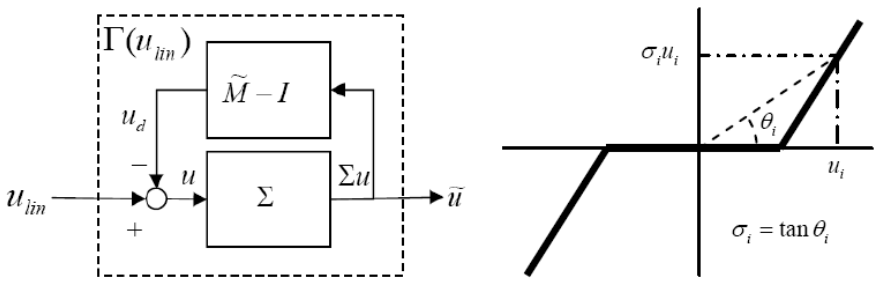

FIGURE 4. The equivalent block diagram of $\Gamma(u_{lin})$ with possible different nonlinearity gains

The robustness of the antiwindup schemes for systems subject to input saturation and coprime factor uncertainties can be obtained from (6), i.e.,

$$\left\|\begin{pmatrix} -M^{-1}\Delta_M & M^{-1}\Delta_N \end{pmatrix}\right\|_\infty < \left\|\begin{pmatrix} I & -\tilde{N}\Gamma_\Sigma \\ 0 & I-\tilde{M}\Gamma_\Sigma \end{pmatrix}\begin{pmatrix} I \\ K_2 \end{pmatrix}(I-G_2K_2)^{-1}\right\|_{i,2}^{-1}$$
$$\leq \left\|\begin{pmatrix} I & -\tilde{N}\Gamma_\Sigma \\ 0 & I-\tilde{M}\Gamma_\Sigma \end{pmatrix}\right\|_{i,2}^{-1} \times \left\|\begin{pmatrix} I \\ K_2 \end{pmatrix}(I-G_2K_2)^{-1}\right\|_\infty^{-1},$$

where $\left\|\begin{pmatrix} I \\ K_2 \end{pmatrix}(I-G_2K_2)^{-1}\right\|_\infty^{-1}$ is the robust bound of the systems without the nonlinearity of the input saturation. $\left\|\begin{pmatrix} I & -\tilde{N}\Gamma_\Sigma \\ 0 & I-\tilde{M}\Gamma_\Sigma \end{pmatrix}\right\|_{i,2}$ results from the input saturation in the robust antiwindup system. From (4), $\left\|\begin{pmatrix} -M^{-1}\Delta_M & M^{-1}\Delta_N \end{pmatrix}\right\|_\infty < \dfrac{1}{\gamma\delta}$, if $\left\|\begin{pmatrix} I & -\tilde{N}\Gamma_\Sigma \\ 0 & I-\tilde{M}\Gamma_\Sigma \end{pmatrix}\right\|_{i,2} < \gamma$. From (5), $I-\tilde{M}\Gamma_\Sigma = (I-\Sigma)(I-\Sigma+\tilde{M}\Sigma)^{-1}$. In case of a special condition that $\Sigma = 0$, $\Gamma_\Sigma = 0$ and $\left\|I-\tilde{M}\Gamma_\Sigma\right\|_{i,2} = \|I\|_\infty = 1$. Then $\left\|I-\tilde{M}\Gamma_\Sigma\right\|_{i,2} \geq 1$ (the same as that in [22]), i.e.,

$$\left\|\begin{pmatrix} I & -\tilde{N}\Gamma_\Sigma \\ 0 & I-\tilde{M}\Gamma_\Sigma \end{pmatrix}\right\|_{i,2} \geq 1. \tag{7}$$

$\begin{pmatrix} I & -\tilde{N}\Gamma_\Sigma \\ 0 & I-\tilde{M}\Gamma_\Sigma \end{pmatrix}$ can be regarded as the penalty operator for the nonlinearity of input saturation and $\gamma > 1$. That is, the antiwindup scheme cannot be expected to have better robustness in nonlinear plants than linear plants. This result is more general for the robust antiwindup synthesis. For instance, there is no penalty for the robustness of the compensated system if the system is linear, or $\Gamma_\Sigma = 0$. In this case, the penalty operator becomes an identity matrix. In case $M^{-1}\Delta_M = 0$, or $\Delta_{G_2} = M^{-1}\Delta_N$, where Δ_{G_2} is defined as the additive plant uncertainty of $\tilde{G}_2$, or $\tilde{G}_2 = G_2 + \Delta_{G_2}$, the robustness requirement of the uncertain system is the same as the result in [22]. Consequently, if $\tilde{G}_2 = G_2 + \Delta_{G_2}$, (6) degenerates into

$$\left\|(I-\tilde{M}\Gamma_\Sigma)K_2(I-G_2K_2)^{-1}\Delta_{G_2}\right\|_{i,2} < 1, \tag{8}$$

or $(I-\tilde{M}\Gamma_\Sigma)$ is the penalty operator of the compensated system subject to input saturation and additive plant uncertainties. Furthermore, if there is no input saturation in the system, or $\Gamma_\Sigma = 0$, (8) also turns into a standard robust control problem with the additive plant uncertainty, i.e., $\|K_2(I-G_2K_2)^{-1}\Delta_{G_2}\|_\infty < 1$.

Table 1 provides the uncertainties I/O gains for the antiwindup scheme with and without input saturation. The robustness criteria of the compensated system will depend on its uncertainty type. For instance, $\left\|(I-\tilde{M}\Gamma_\Sigma)K_2(I-G_2K_2)^{-1}\right\|_{i,2}^{-1}$ and $\left\|\begin{pmatrix} I & -\tilde{N}\Gamma_\Sigma \\ 0 & I-\tilde{M}\Gamma_\Sigma \end{pmatrix}\begin{pmatrix} I \\ K_2 \end{pmatrix}(I-G_2K_2)^{-1}\right\|_{i,2}^{-1}$ are the different robustness criteria of the compensated system for the antiwindup scheme with the additive uncertainty and the coprime factor uncertainties, respectively. According to the different robustness criteria, it can conclude that

one compensator which may be better than the other compensator for a kind of robustness criteria is not always better for other kinds of robustness criteria.

TABLE 1. Uncertainty I/O gains for the antiwindup scheme

Model uncertainty type	Plant with additive uncertainty		Plant with coprime factor uncertainties	
Input saturation	No	Yes	No	Yes
Uncertainties I/O gain	$K_2(I-G_2K_2)^{-1}$	$(I-\tilde{M}\Gamma_\Sigma)K_2(I-G_2K_2)^{-1}$	$\begin{pmatrix} I \\ K_2 \end{pmatrix}(I-G_2K_2)^{-1}$	$\begin{pmatrix} I & -\tilde{N}\Gamma_\Sigma \\ 0 & I-\tilde{M}\Gamma_\Sigma \end{pmatrix}\begin{pmatrix} I \\ K_2 \end{pmatrix}(I-G_2K_2)^{-1}$

4. **The Stability Robustness of the Compensated System.** The block with dash-dot border in Figure 3 shows the mapping of the penalty operator since

$$\begin{pmatrix} y_G \\ u_{lin} \end{pmatrix} = \begin{pmatrix} -(I-G_2K_2)^{-1} & (I-G_2K_2)^{-1} \\ -K_2(I-G_2K_2)^{-1} & K_2(I-G_2K_2)^{-1} \end{pmatrix} \begin{pmatrix} u_M \\ u_N \end{pmatrix},$$

or $y_G = G_2u_{lin} - u_M + u_N$. Figure 5 is the equivalent block diagram of the penalty operator for the input saturation with coprime factor uncertainties. Thus, $\begin{pmatrix} y_M \\ y_N \end{pmatrix} = \begin{pmatrix} y_G - \tilde{N}\tilde{u} \\ u_{lin} - \tilde{M}\tilde{u} \end{pmatrix}$, or equivalently,

$$\begin{pmatrix} y_M \\ y_N \end{pmatrix} = \begin{pmatrix} G_2u_{lin} - u_M + u_N - \tilde{N}\tilde{u} \\ u_{lin} - \tilde{M}\tilde{u} \end{pmatrix}. \tag{9}$$

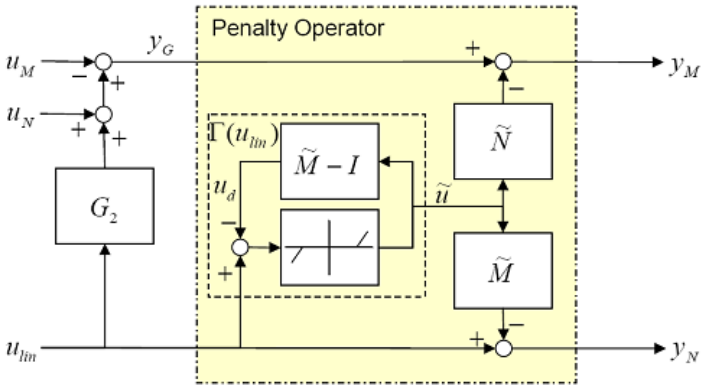

FIGURE 5. Block diagram of the penalty operator $\begin{pmatrix} I & -\tilde{N}\Gamma_\Sigma \\ 0 & I-\tilde{M}\Gamma_\Sigma \end{pmatrix}$ from $\begin{pmatrix} y_G \\ u_{lin} \end{pmatrix}$ to $\begin{pmatrix} y_M \\ y_N \end{pmatrix}$

According to (2) and (3), the state equations of (9) can be as follows.

$$\dot{x}_1 = (A+BF)x_1 + B\tilde{u} \tag{10}$$

$$\dot{x}_2 = Ax_2 + Bu_{lin}. \tag{11}$$

Then

$$y_G = Cx_2 + Du_{lin} - u_M + u_N. \tag{12}$$

In addition, some necessary outputs for the antiwindup synthesis are as follows.

$$y_M = -(C + DF)x_1 + Cx_2 - D\tilde{u} + Du_{lin} - u_M + u_N, \tag{13}$$
$$y_N = -Fx_1 - \tilde{u} + u_{lin}, \tag{14}$$
$$u_d = Fx_1, \tag{15}$$
$$y_d = (C + DF)x_1 + D\tilde{u}. \tag{16}$$

The criterion for stability robustness optimization has been proposed for systems with both input saturation and additive plant uncertainties in [22]. Similarly, the compensated system can be guaranteed to be robustly stable for a plant with the coprime factor uncertainty matrix $\begin{pmatrix} -M^{-1}\Delta_M & M^{-1}\Delta_N \end{pmatrix}$, the dead-zone nonlinearity constraint [27], $\tilde{u}^T\Lambda(u_{lin} - u_d - \tilde{u}) \geq 0$, and the induced L_2-norm of the penalty operator

$$\left\| \begin{pmatrix} I & -\tilde{N}\Gamma_\Sigma \\ 0 & I - \tilde{M}\Gamma_\Sigma \end{pmatrix} \right\|_{i,2} < \gamma,$$

if

$$J_R = \frac{d}{dt}\left(x^T P x\right) + \left\| \begin{pmatrix} y_M \\ y_N \end{pmatrix} \right\|^2 - \gamma^2 \left\| \begin{pmatrix} y_G \\ u_{lin} \end{pmatrix} \right\|^2 + 2\tilde{u}^T\Lambda(u_{lin} - u_d - \tilde{u}) < 0, \tag{17}$$

where $P > 0$ and $\Lambda \equiv diag(\lambda_1, \cdots, \lambda_q) > 0$. (17) shows the robustness requirement for input saturation with coprime factor uncertainties. The terms $\left\| \begin{pmatrix} y_M \\ y_N \end{pmatrix} \right\|^2 - \gamma^2 \left\| \begin{pmatrix} y_G \\ u_{lin} \end{pmatrix} \right\|^2$ in Equation (17) represented the effects of the induced L_2-norm of the penalty operator, $\left\| \begin{pmatrix} I & -\tilde{N}\Gamma_\Sigma \\ 0 & I - \tilde{M}\Gamma_\Sigma \end{pmatrix} \right\|_{i,2} < \gamma$, since the nonlinear operators of either Γ_Σ or the penalty operator cannot be simply realized. Furthermore, $\begin{pmatrix} y_M \\ y_N \end{pmatrix}$ in (9) is in terms of the inputs $\tilde{u}$, u_{lin}, u_M and u_N, exclusive of $\Gamma(u_{lin})$. That is, $\tilde{u}$, (the output of $\Gamma(u_{lin})$) is independent of u_{lin} (the input of $\Gamma(u_{lin})$) whatever $\Gamma(u_{lin})$ is. It is obvious that $\tilde{u}^T\Lambda(u_{lin} - u_d - \tilde{u})$ is equal to zero in the linear zones of inputs and is greater than zero in the input saturation zones. Theorem 4.1 gives the LMI constraint of the robust stability for the antiwindup scheme.

Theorem 4.1. *The antiwindup compensator guarantees the robustness stability of the compensated system subject to the input saturation and the coprime factor uncertainty matrix* $(-M^{-1}\Delta_M, M^{-1}\Delta_N)$ *as shown in Figure 2 if the matrices* $P = \begin{pmatrix} P_1 & P_3 \\ P_3^T & P_2 \end{pmatrix} > 0$, $\Lambda \equiv diag(\lambda_1, \cdots, \lambda_q) > 0$, *and* F *satisfy the following LMI.*

$$\begin{pmatrix} (A+BF)^T P_1 + P_1(A+BF) & (A+BF)^T P_3 + P_3 A & P_1 B - F^T\Lambda \\ * & A^T P_2 + P_2 A - \gamma^2 C^T C & P_3^T B \\ * & * & -2\Lambda \\ * & * & * \\ * & * & * \\ * & * & * \\ * & * & * \end{pmatrix}$$

$$\begin{pmatrix} P_3B & 0 & (C+DF)^T & F^T \\ P_2B-\gamma^2C^TD & -\gamma^2C^T & -C^T & 0 \\ \Lambda & 0 & D^T & I \\ -\gamma^2(D^TD+I) & -\gamma^2D^T & -D^T & -I \\ * & -\gamma^2I & -I & 0 \\ * & * & -I & 0 \\ * & * & * & -I \end{pmatrix} < 0. \tag{18}$$

Proof: From (10)-(15), (17) becomes

$$J_R = \begin{pmatrix} x_1 \\ x_2 \\ \tilde{u} \\ u_{lin} \\ u_N - u_M \end{pmatrix}^T \Re_R \begin{pmatrix} x_1 \\ x_2 \\ \tilde{u} \\ u_{lin} \\ u_N - u_M \end{pmatrix} < 0.$$

Thus

$$\Re_R = \begin{pmatrix} (A+BF)^TP_1+P_1(A+BF)+F^TF+(C+DF)^T(C+DF) & (A+BF)^TP_3+P_3A-(C+DF)^TC \\ * & A^TP_2+P_2A-\gamma^2C^TC+C^TC \\ * & * \\ * & * \\ * & * \end{pmatrix}$$
$$\begin{pmatrix} P_1B-F^T\Lambda+F^T+(C+DF)^TD & P_3B-F^T-(C+DF)^TD & -(C+DF)^T \\ P_3^TB-C^TD & P_2B-\gamma^2C^TD+C^TD & (1-\gamma^2)C^T \\ -2\Lambda+I+D^TD & \Lambda-I-D^TD & -D^T \\ * & (1-\gamma^2)(I+D^TD) & (1-\gamma^2)D^T \\ * & * & (1-\gamma^2)I \end{pmatrix}$$
$$\underline{\underline{SC}} \begin{pmatrix} (A+BF)^TP_1+P_1(A+BF)+F^TF & (A+BF)^TP_3+P_3A & P_1B-F^T\Lambda+F^T \\ * & A^TP_2+P_2A-\gamma^2C^TC & P_3^TB \\ * & * & -2\Lambda+I \\ * & * & * \\ * & * & * \\ * & * & * \end{pmatrix}$$
$$\begin{pmatrix} P_3B-F^T & 0 & (C+DF)^T \\ P_2B-\gamma^2C^TD & -\gamma^2C^T & -C^T \\ \Lambda-I & 0 & D^T \\ -\gamma^2(D^TD+I)+I & -\gamma^2D^T & -D^T \\ * & -\gamma^2I & -I \\ * & * & -I \end{pmatrix}$$
$$\underline{\underline{SC}} \begin{pmatrix} (A+BF)^TP_1+P_1(A+BF) & (A+BF)^TP_3+P_3A & P_1B-F^T\Lambda \\ * & A^TP_2+P_2A-\gamma^2C^TC & P_3^TB \\ * & * & -2\Lambda \\ * & * & * \\ * & * & * \\ * & * & * \\ * & * & * \end{pmatrix}$$
$$\begin{pmatrix} P_3B & 0 & (C+DF)^T & F^T \\ P_2B-\gamma^2C^TD & -\gamma^2C^T & -C^T & 0 \\ \Lambda & 0 & D^T & I \\ -\gamma^2(D^TD+I) & -\gamma^2D^T & -D^T & -I \\ * & -\gamma^2I & -I & 0 \\ * & * & -I & 0 \\ * & * & * & -I \end{pmatrix} < 0.$$

Since the LMI in (18) holds, (17) will be satisfied and the compensated system is stable in the presence of the coprime factor uncertainties and input saturation nonlinearity. Hence, the robust bound of the compensated system, $\left\| \begin{pmatrix} -M^{-1}\Delta_M & M^{-1}\Delta_N \end{pmatrix} \right\|_\infty$, is less than $\dfrac{1}{\gamma\delta}$. The diagonal terms of the matrices during the derivations of the proof are all negative definite. These terms also represent the necessary conditions of the LMI in

(18). Therefore, $\gamma > 1$. This result is the same as anticipated in (7). These necessary conditions are helpful to assess the satisfaction of (12). If $P = \begin{pmatrix} P_1 & 0 \\ 0 & P_2 \end{pmatrix} > 0$, or $P_3 = 0$, and after the congruence transformation $diag\,(Q_1, I, V, I, I, I, I)$, (18) becomes

$$\Re_R \underset{Q_1,I,V,I,I,I}{\overset{CT}{=\!=\!=}} \begin{pmatrix} Q_1A^T + AQ_1 + L^TB^T + BL & 0 & BV - L^T \\ * & A^TP_2 + P_2A - \gamma^2C^TC & 0 \\ * & * & -2V \\ * & * & * \\ * & * & * \\ * & * & * \\ * & * & * \end{pmatrix}$$

$$\begin{pmatrix} 0 & Q_1C^T + L^TD^T & L^T & 0 \\ P_2B - \gamma^2C^TD & -C^T & 0 & -\gamma^2C^T \\ I & VD^T & V & 0 \\ -\gamma^2(D^TD + I) & -D^T & -I & -\gamma^2D^T \\ * & -I & 0 & -I \\ * & * & -I & 0 \\ * & * & * & -\gamma^2I \end{pmatrix} < 0, \tag{19}$$

where $Q_1 = P_1^{-1}$, $L = FQ_1$ and $V = \Lambda^{-1}$. LMI in (19) ensures the robustness requirement of the compensated system subject to input saturation and the coprime factor uncertainties. The antiwindup compensator can be found, i.e., $F = LQ_1^{-1}$. The state space representation of the antiwindup compensator can be written as

$$\begin{pmatrix} \tilde{M} - I \\ \tilde{N} \end{pmatrix} \overset{S}{=} \left[\begin{array}{c|c} A + BLQ_1^{-1} & B \\ \hline LQ_1^{-1} & 0 \\ C + DLQ_1^{-1} & D \end{array}\right]. \tag{20}$$

5. **The Robustness and Performance of the Compensated System.** The antiwindup compensator is expected to maintain the performance of a linear control system subject to input saturation while guaranteeing the global stability or minimizing performance deterioration. However, (17) cannot guarantee the performance of the compensated system. The criterion of the optimization for the robustness and performance was proposed in [20] and can be adopted in this paper, i.e.,

$$J_p = \frac{d}{dt}\left(x^TPx\right) + \left\| \begin{pmatrix} W_P^{\frac{1}{2}}y_d \\ W_{RM}^{\frac{1}{2}}y_M \\ W_{RN}^{\frac{1}{2}}y_N \end{pmatrix} \right\|^2 - \gamma^2 \left\| \begin{pmatrix} y_G \\ u_{lin} \end{pmatrix} \right\|^2 + 2\tilde{u}^T\Lambda(u_{lin} - u_d - \tilde{u}) < 0, \tag{21}$$

where W_P, W_{RM} and W_{RN} are the weighting matrices for the performance and robustness of coprime factors, respectively, and

$$\left\| \begin{pmatrix} W_P^{\frac{1}{2}}y_d \\ W_{RM}^{\frac{1}{2}}y_M \\ W_{RN}^{\frac{1}{2}}y_N \end{pmatrix} \right\|^2 < \gamma^2 \left\| \begin{pmatrix} y_G \\ u_{lin} \end{pmatrix} \right\|^2. \tag{22}$$

W_P, W_{RM} and W_{RN} can reveal the relative significance of performance or robustness in the antiwindup synthesis. For instance, if W_P is equal to zero or a small value compared with those of W_{RM} and W_{RN}, the robustness of the antiwindup system is more important than the performance. The optimization for J_p will degenerate into the robustness optimization as in Theorem 4.1. Similarly, if W_{RM} and W_{RN} are chosen small compared with

that of W_P, the antiwindup system performance is more significant than the robustness. In Theorem 5.1, (21) can be formulated using LMI through some Schur complement operations and congruence transformations for any possible relative significance of performance and robustness.

Theorem 5.1. *The antiwindup compensator will guarantee the robustness stability and the performance of the closed-loop system in the presence of input saturation and the coprime factor uncertainty matrix* $\begin{pmatrix} -M^{-1}\Delta_M & M^{-1}\Delta_N \end{pmatrix}$ *if (22) holds as well as the matrices* $P = \begin{pmatrix} P_1 & P_3 \\ P_3^T & P_2 \end{pmatrix} > 0$, $\Lambda \equiv diag(\lambda_1, \cdots, \lambda_q) > 0$, *and* F *exist such that the following LMI is satisfied.*

$$\begin{pmatrix} (A+BF)^TP_1 + P_1(A+BF) & (A+BF)^TP_3 + P_3A & P_1B - F^T\Lambda \\ * & A^TP_2 + P_2A - \gamma^2C^TC & P_3^TB \\ * & * & -2\Lambda \\ * & * & * \\ * & * & * \\ * & * & * \\ * & * & * \\ * & * & * \end{pmatrix}$$

$$\begin{pmatrix} P_3B & 0 & (C+DF)^T & F^T & (C+DF)^T \\ P_2B - \gamma^2C^TD & -\gamma^2C^T & -C^T & 0 & 0 \\ \Lambda & 0 & D^T & I & D^T \\ -\gamma^2(I + D^TD) & -\gamma^2D^T & -D^T & -I & 0 \\ * & -\gamma^2I & -I & 0 & 0 \\ * & * & -W_{RM}^{-1} & 0 & 0 \\ * & * & * & -W_{RN}^{-1} & 0 \\ * & * & * & * & -W_P^{-1} \end{pmatrix} < 0. \tag{23}$$

Proof: Following the similar procedure in the proof of Theorem 4.1 including (16), we have

$$J_P = \begin{pmatrix} x_1 \\ x_2 \\ \tilde{u} \\ u_{lin} \\ u_N - u_M \end{pmatrix}^T \Re_P \begin{pmatrix} x_1 \\ x_2 \\ \tilde{u} \\ u_{lin} \\ u_N - u_M \end{pmatrix} < 0,$$

where

$$\Re_P = \begin{pmatrix} (A+BF)^TP_1 + P_1(A+BF) + F^TW_{RN}F + (C+DF)^T(W_P + W_{RM})(C+DF) & \\ * & \\ * & \\ * & \\ * & \end{pmatrix}$$

$$\begin{matrix} (A+BF)^TP_3 + P_3A - (C+DF)^TW_{RM}C & P_1B - F^T\Lambda + F^TW_{RN} + (C+DF)^T(W_P + W_{RM})D \\ A^TP_2 + P_2A - \gamma^2C^TC + C^TW_{RM}C & P_3^TB - C^TW_{RM}D \\ * & -2\Lambda + W_{RN} + D^T(W_P + W_{RM})D \\ * & * \\ * & * \end{matrix}$$

$$\left.\begin{matrix} P_3B - F^TW_{RN} - (C+DF)^TW_{RM}D & -(C+DF)^TW_{RM} \\ P_2B - \gamma^2C^TD + C^TW_{RM}D & C^T(W_{RM}-\gamma^2 I) \\ \Lambda - W_{RN} - D^TW_{RM}D & -D^TW_{RM} \\ W_{RN} + D^TW_{RM}D - \gamma^2(I+D^TD) & D^T(W_{RM}-\gamma^2 I) \\ * & (W_{RM}-\gamma^2 I) \end{matrix}\right). \tag{24}$$

Applying some Schur complement operations and the congruence transformation $diag\left(I, I, I, I, I, W_{RM}^{-\frac{1}{2}}, W_{RN}^{-\frac{1}{2}}, W_P^{-\frac{1}{2}}\right)$, the LMI can be as follows:

$$\Re_P \overset{CT}{\underset{I,I,I,I,I,W_{RM}^{-\frac{1}{2}},W_{RN}^{-\frac{1}{2}},W_P^{-\frac{1}{2}}}{=\!=\!=}} \left(\begin{matrix} (A+BF)^TP_1 + P_1(A+BF) & (A+BF)^TP_3 + P_3A & P_1B - F^T\Lambda \\ * & A^TP_2 + P_2A - \gamma^2C^TC & P_3^TB \\ * & * & -2\Lambda \\ * & * & * \\ * & * & * \\ * & * & * \\ * & * & * \\ * & * & * \end{matrix}\right.$$

$$\left.\begin{matrix} P_3B & 0 & (C+DF)^T & F^T & (C+DF)^T \\ P_2B - \gamma^2C^TD & -\gamma^2C^T & -C^T & 0 & 0 \\ \Lambda & 0 & D^T & I & D^T \\ -\gamma^2(I+D^TD) & -\gamma^2D^T & -D^T & -I & 0 \\ * & -\gamma^2 I & -I & 0 & 0 \\ * & * & -W_{RM}^{-1} & 0 & 0 \\ * & * & * & -W_{RN}^{-1} & 0 \\ * & * & * & * & -W_P^{-1} \end{matrix}\right).$$

(23) can be proven.

From (22), the necessary condition of the robustness is

$$\left\|\begin{pmatrix} I & -\tilde{N}\Gamma_\Sigma \\ 0 & I-\tilde{M}\Gamma_\Sigma \end{pmatrix}\begin{pmatrix} W_{RM}^{\frac{1}{2}} & 0 \\ 0 & W_{RN}^{\frac{1}{2}} \end{pmatrix}\right\|_{i,2} < \gamma,$$

i.e.,

$$\left\|\begin{pmatrix} I & -\tilde{N}\Gamma_\Sigma \\ 0 & I-\tilde{M}\Gamma_\Sigma \end{pmatrix}\right\|_{i,2} < \frac{\gamma}{\sqrt{\underline{\sigma}\begin{pmatrix} W_{RM} & 0 \\ 0 & W_{RN} \end{pmatrix}}}.$$

In (4,4) block of (24), $\begin{pmatrix} W_{RM} & 0 \\ 0 & W_{RN} \end{pmatrix} < \gamma^2 I$, or equivalently, $\frac{\gamma}{\sqrt{\underline{\sigma}\begin{pmatrix} W_{RM} & 0 \\ 0 & W_{RN} \end{pmatrix}}} > 1$. In other words, the antiwindup scheme cannot be expected to have better robustness for nonlinear plants than that for linear plants in either the stability robustness or the robustness and performance of the compensated system. We can also suggest that $P = \begin{pmatrix} P_1 & 0 \\ 0 & P_2 \end{pmatrix} > 0$, or $P_3 = 0$. In this case, (23) becomes

$$\Re_P \overset{CT}{\underset{Q_1,I,V,I,I,I,I,I}{=\!=\!=}} \left(\begin{matrix} Q_1A^T + AQ_1 + L^TB^T + BL & 0 & BV - L^T \\ * & A^TP_2 + P_2A - \gamma^2C^TC & 0 \\ * & * & -2V \\ * & * & * \\ * & * & * \\ * & * & * \\ * & * & * \\ * & * & * \end{matrix}\right.$$

$$\begin{pmatrix} 0 & 0 & Q_1C^T + L^TD^T & L^T & Q_1C^T + L^TD^T \\ P_2B - \gamma^2 C^TD & -\gamma^2 C^T & -C^T & 0 & 0 \\ I & 0 & VD^T & V & VD^T \\ -\gamma^2(I + D^TD) & -\gamma^2 D^T & -D^T & -I & 0 \\ * & -\gamma^2 I & -I & 0 & 0 \\ * & * & -W_{RM}^{-1} & 0 & 0 \\ * & * & * & -W_{RN}^{-1} & 0 \\ * & * & * & * & -W_P^{-1} \end{pmatrix} < 0, \qquad (25)$$

where $Q_1 = P_1^{-1}$, $L = FQ_1$ and $V = \Lambda^{-1}$. The antiwindup compensator which guarantees the robustness stability and the performance of the closed-loop system as specified in (22) can be synthesized, i.e., $F = LQ_1^{-1}$, where L satisfies the LMI in (25). Furthermore, its state space representation is similar to (20).

6. **Examples.** Example 6.1 accounts for the differences in the robustness criteria between the additive uncertainty and the coprime factor uncertainties. The robustness analysis involves the maximal singular values of the uncertainty I/O map. Two different feedback compensators provide the typical robustness measurements for both kinds of uncertainties. Examples 6.2 and 6.3 that have been carried out in [22] demonstrate the implications of the LMI approach to the antiwindup synthesis proposed in this paper. Furthermore, the time responses of two more perturbed plants which are both unstable are utilized to compare the robustness of the antiwindup compensators in [22] with that in this paper. Example 6.4 presents the antiwindup synthesis for a rotorcraft model in hover flight condition. It illustrates the proposed approach applied to a practical system.

Example 6.1. *Consider the following multivariable system. The state-space matrix of the plant is described as follows.*

$$G_2 \stackrel{s}{=} \left[\begin{array}{cc|cc} -0.0250 & 0.0750 & 4.4000 & 4.2800 \\ 0.0750 & -0.0250 & 5.6000 & 5.7200 \\ \hline 0.0150 & 0.0050 & 0.0500 & 0.0600 \\ 0.6500 & 0.0500 & 3.0000 & 3.6000 \end{array}\right].$$

Two possible feedback compensators that stabilize G_2 are respectively described by the state-space matrices

$$K_2 \stackrel{s}{=} \left[\begin{array}{cc|cc} -3.1390 & -0.3453 & 0.02528 & 0.8622 \\ -4.0810 & -0.5892 & 0.03005 & 0.9999 \\ \hline -10.59 & -1.666 & -0.0500 & -3.0000 \\ -10.38 & -1.640 & -0.0600 & -3.6000 \end{array}\right]$$

and

$$\bar{K}_2 \stackrel{s}{=} \left[\begin{array}{cc|cc} -0.08834 & 0.03105 & -0.0009227 & -0.03230 \\ 0.02173 & -0.08151 & 0.0001539 & 0.005388 \\ \hline 0.01381 & 0.005244 & 0.0004078 & 0.01427 \\ 0.01381 & 0.005244 & 0.0004078 & 0.01427 \end{array}\right].$$

Figure 6 plots the maximal singular values of the uncertainty I/O maps for the closed-loop systems with K_2 and $\bar{K}_2$. Figure 6(a) illustrates that the robustness of the closed-loop system with $\bar{K}_2$ is better than that with K_2 for the additive uncertainty since $\left\|\bar{K}_2(I - G_2\bar{K}_2)^{-1}\right\|_\infty = 0.0223$ and $\|K_2(I - G_2K_2)^{-1}\|_\infty = 0.2041$. From the small gain theorem, the uncertainty bounds of the stability for the additive uncertainty are 44.8505 and 4.8746 with the compensators $\bar{K}_2$ and K_2, respectively. However, Figure 6(b) shows that $\left\|\begin{pmatrix} I \\ \bar{K}_2 \end{pmatrix}(I - G_2\bar{K}_2)^{-1}\right\|_\infty = 1.10429$ and $\left\|\begin{pmatrix} I \\ K_2 \end{pmatrix}(I - G_2K_2)^{-1}\right\|_\infty = 1.00003$.

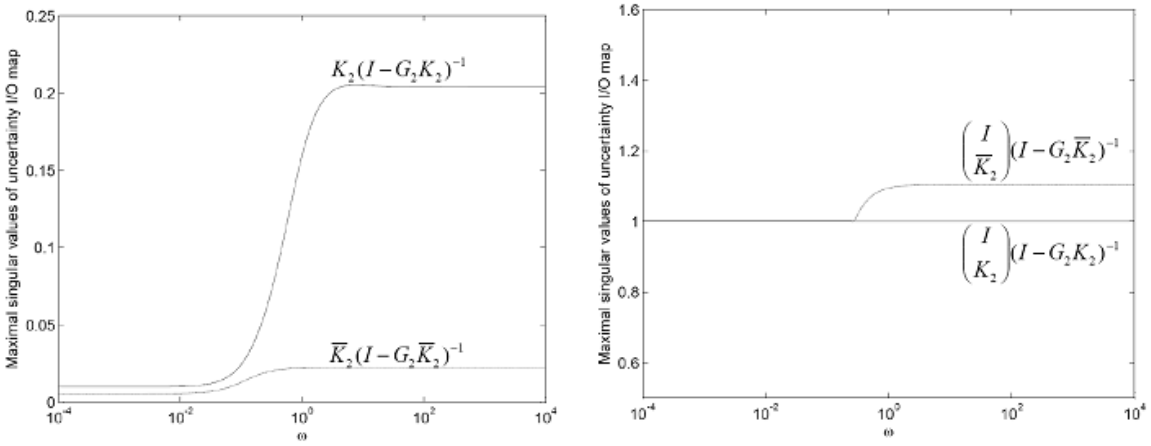

(a) The additive uncertainty I/O maps (b) The coprime factor uncertainty I/O maps

FIGURE 6. The maximal singular values for uncertainty I/O maps

That is, similarly from small gain theorem, the robustness for the coprime factor uncertainties with K_2 is better than that with $\bar{K}_2$. According to the above analysis, there is no obvious correlation for robustness between the additive uncertainty and the coprime factor uncertainties. As a result, one compensator that may be better for one kind of uncertainties is not always better for the other kind of uncertainties.

Example 6.2. *Consider the benchmark example in [22]. The nominal plant, G_2, described by the state-space matrix is as follows.*

$$G_2 \overset{S}{=} \left[\begin{array}{cc|c} 0 & 1 & 0 \\ -10 & -10 & 10 \\ \hline 1 & 0 & 0 \end{array}\right].$$

Three perturbed plants are utilized to compare the time responses of the compensated systems between compensators in this paper. Their state-space matrices are described as follows.

Perturbed Plant 1: $G_{2P1} \overset{S}{=} \left[\begin{array}{cc|c} 0 & 1 & 0 \\ -10 & -0.01 & 10 \\ \hline 1 & 0 & 0 \end{array}\right]$;

Perturbed Plant 2: $G_{2P2} \overset{S}{=} \left[\begin{array}{cc|c} 0 & 1 & 0 \\ -10 & 0.44 & 10 \\ \hline 1 & 0 & 0 \end{array}\right]$;

Perturbed Plant 3: $G_{2P3} \overset{S}{=} \left[\begin{array}{cc|c} 0 & 1 & 0 \\ -10 & 0.45 & 10 \\ \hline 1 & 0 & 0 \end{array}\right]$.

Perturbed Plant 1 is the same as that in [22]. Perturbed Plants 2 and 3 are both unstable. The feedback controller, K, which was designed for G_2 is described as

$$K = \begin{pmatrix} K_1 & K_2 \end{pmatrix} \overset{S}{=} \left[\begin{array}{ccc|cc} -80 & 0 & 2.5 & 0 & -1 \\ 1 & 0 & 0 & 0 & 0 \\ 0 & 0 & -2.5 & 1 & 0 \\ \hline -9450 & 3375 & 337.5 & 0 & -135 \end{array}\right].$$

With claim to robustness of the system in [22], the full order antiwindup compensator was synthesized as

$$\begin{pmatrix} \bar{\tilde{M}}_R - I \\ \bar{\tilde{N}}_R \end{pmatrix} \overset{s}{=} \left[\begin{array}{cc|c} 0 & 1 & 0 \\ -9.9998 & -10.0000 & 10 \\ \hline 0.00002242 & 0.00000446 & 0 \\ 1 & 0 & 0 \end{array}\right],$$

where $\bar{F}_R = \begin{pmatrix} 0.2242 & 0.0446 \end{pmatrix} \times 10^{-4}$, and the weighting matrices $W_p = 0.001$ and $W_r = 1$. The robustness of the antiwindup synthesis in this example is more significant than performance. In this paper, we similarly choose $W_P = 0.001$, $W_{RM} = 1$ and $W_{RN} = 1$. According to (25), $F_R = \begin{pmatrix} 0.001382 & 0.001560 \end{pmatrix}$. The antiwindup compensator can be

$$\begin{pmatrix} \tilde{M}_R - I \\ \tilde{N}_R \end{pmatrix} \overset{s}{=} \left[\begin{array}{cc|c} 0 & 1 & 0 \\ -9.9861 & -9.9844 & 10 \\ \hline 0.001382 & 0.001560 & 0 \\ 1 & 0 & 0 \end{array}\right].$$

TABLE 2. The induced L_2-norms of I/O maps with different Σ in Example 6.2

Σ	$0.3I$	$0.6I$	$0.9I$
$\left\|(I - \tilde{M}\Gamma_\Sigma)K_2(I - G_2K_2)^{-1}\right\|_{i,2}$	94.4983	53.9990	13.4998
$\left\|(I - \bar{\tilde{M}}\Gamma_\Sigma)K_2(I - G_2K_2)^{-1}\right\|_{i,2}$	94.4983	53.9990	13.4998
$\left\|(I - \bar{\tilde{M}}\Gamma_\Sigma)K_2(I - G_2K_2)^{-1}\right\|_{i,2} - \left\|(I - \tilde{M}\Gamma_\Sigma)K_2(I - G_2K_2)^{-1}\right\|_{i,2}$	4.0186×10^{-8}	4.5939×10^{-8}	1.7232×10^{-8}
$\left\|\begin{pmatrix} I & -\tilde{N}\Gamma_\Sigma \\ 0 & I - \tilde{M}\Gamma_\Sigma \end{pmatrix}\begin{pmatrix} I \\ K_2 \end{pmatrix}(I - G_2K_2)^{-1}\right\|_{i,2}$	94.5036	54.0083	13.5367
$\left\|\begin{pmatrix} I & -\bar{\tilde{N}}\Gamma_\Sigma \\ 0 & I - \bar{\tilde{M}}\Gamma_\Sigma \end{pmatrix}\begin{pmatrix} I \\ K_2 \end{pmatrix}(I - G_2K_2)^{-1}\right\|_{i,2}$	94.5036	54.0083	13.5367
$\left\|\begin{pmatrix} I & -\bar{\tilde{N}}\Gamma_\Sigma \\ 0 & I - \bar{\tilde{M}}\Gamma_\Sigma \end{pmatrix}\begin{pmatrix} I \\ K_2 \end{pmatrix}(I - G_2K_2)^{-1}\right\|_{i,2} - \left\|\begin{pmatrix} I & -\tilde{N}\Gamma_\Sigma \\ 0 & I - \tilde{M}\Gamma_\Sigma \end{pmatrix}\begin{pmatrix} I \\ K_2 \end{pmatrix}(I - G_2K_2)^{-1}\right\|_{i,2}$	4.0184×10^{-8}	4.5931×10^{-8}	1.7184×10^{-8}

The antiwindup compensator does not influence the system within the linear zone, or as $\Sigma = 0$. The robustness of the compensated system depends on K_2 only as $\Sigma = 0$ (refer to Table 1). Table 2 compares the induced L_2-norms of I/O maps for the additive uncertainty and coprime factor uncertainties with different Σ. The robustness has no significant differences between these two antiwindup compensators. In fact, the robustness of the antiwindup compensator synthesized in this paper is little better than that in [22] both for the additive uncertainty and the coprime factor uncertainties as shown in Table 2 since $\left\|(I - \bar{\tilde{M}}\Gamma_\Sigma)K_2(I - G_2K_2)^{-1}\right\|_{i,2} > \left\|(I - \tilde{M}\Gamma_\Sigma)K_2(I - G_2K_2)^{-1}\right\|_{i,2}$ and $\left\|\begin{pmatrix} I & -\bar{\tilde{N}}\Gamma_\Sigma \\ 0 & I - \bar{\tilde{M}}\Gamma_\Sigma \end{pmatrix}\begin{pmatrix} I \\ K_2 \end{pmatrix}(I - G_2K_2)^{-1}\right\|_{i,2} > \left\|\begin{pmatrix} I & -\tilde{N}\Gamma_\Sigma \\ 0 & I - \tilde{M}\Gamma_\Sigma \end{pmatrix}\begin{pmatrix} I \\ K_2 \end{pmatrix}(I - G_2K_2)^{-1}\right\|_{i,2}$ for all different Σ. In general, the control input is assumed to be saturated at ± 1. Figure 7 shows the time responses of the compensated systems (including G_2, G_{2P1}, G_{2P2} and G_{2P3}) with the above two antiwindup compensators to a pulse reference of magnitude 1.2. The pulse reference has the same pattern in [22]. The output time responses for these two compensators are almost the same as well in Figure 7. The performance of the antiwindup compensators in this paper are close to that in [22] in both frequency domain and time

domain for either the nominal plant or the perturbed plants when the robustness is more significant than performance.

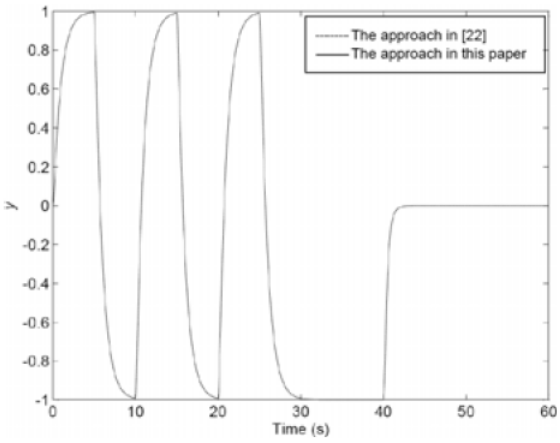

(a) Nominal Plant

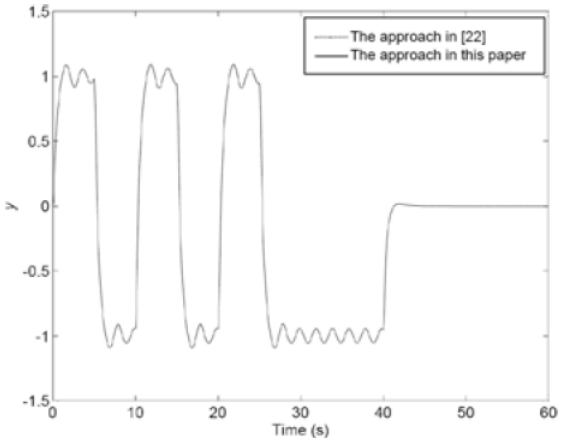

(b) Perturbed Plant 1

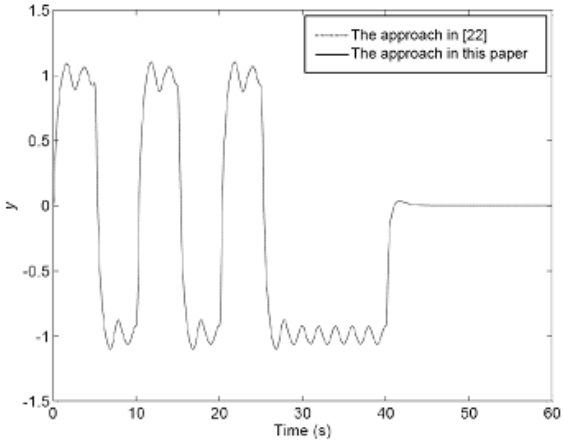

(c) Perturbed Plant 2

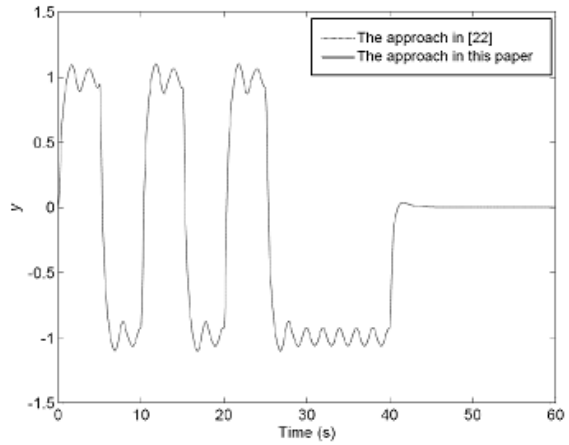

(d) Perturbed Plant 3

FIGURE 7. Output time responses of plants with $W_P = 0.001$, $W_{RM} = 1$ and $W_{RN} = 1$

Example 6.3. *This example emphasizes the performance rather than robustness of the closed-loop system. The nominal plant and the perturbed plants considered are the same as Example 6.2. In [22],* $\bar{F}_P = \begin{pmatrix} -13138 & -1424 \end{pmatrix}$ *as the weighting matrices* $W_p = 1$ *and* $W_r = 0.0001$*. It yields the full-order antiwindup compensator described as*

$$\begin{pmatrix} \bar{\tilde{M}}_P - I \\ \bar{\tilde{N}}_P \end{pmatrix} \stackrel{s}{=} \left[\begin{array}{cc|c} 0 & 1 & 0 \\ -131390 & -14250 & 10 \\ \hline -13138 & -1424 & 0 \\ 1 & 0 & 0 \end{array}\right].$$

According to the proposed approach in this paper in (25), $F_P = \begin{pmatrix} 0.1794 & 0.2101 \end{pmatrix}$ *with* $W_P = 1$*,* $W_{RM} = 0.0001$ *and* $W_{RN} = 0.0001$*. A full-order antiwindup compensator is*

synthesized as follows.

$$\begin{pmatrix} \tilde{M}_P - I \\ \tilde{N}_P \end{pmatrix} \stackrel{S}{=} \left[\begin{array}{cc|c} 0 & 1 & 0 \\ -8.2061 & -7.8992 & 10 \\ \hline 0.1794 & 0.2101 & 0 \\ 1 & 0 & 0 \end{array}\right].$$

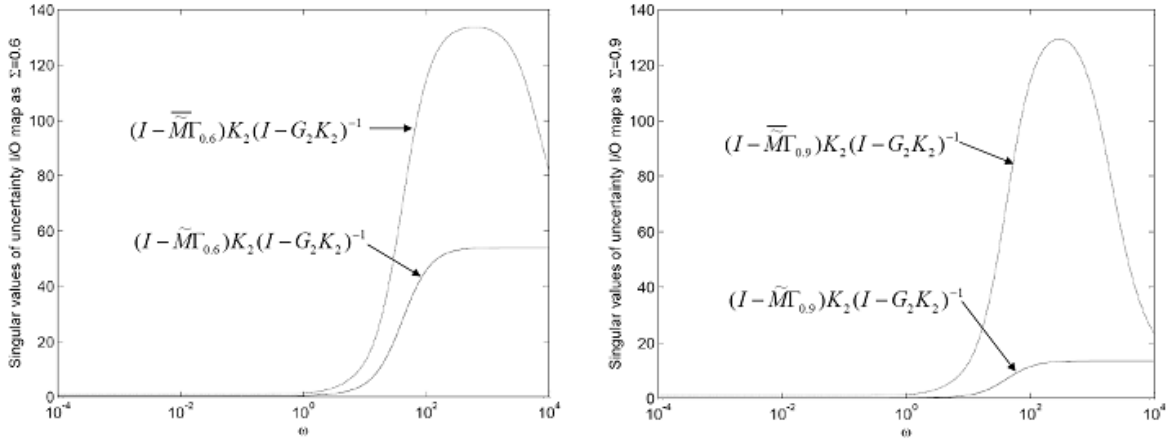

(a) $\Sigma = 0.6$ (b) $\Sigma = 0.9$

FIGURE 8. The singular values of $(I-\tilde{M}\Gamma_\Sigma)K_2(I-G_2K_2)^{-1}$ for the additive uncertainty with $W_P = 1$, $W_{RM} = 0.0001$ and $W_{RN} = 0.0001$

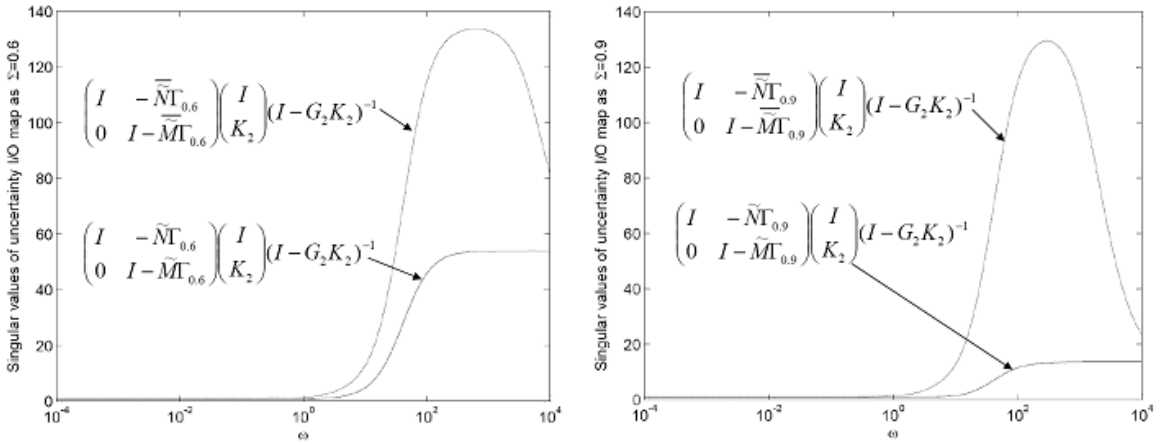

(a) $\Sigma = 0.6$ (b) $\Sigma = 0.9$

FIGURE 9. The singular values of $\begin{pmatrix} I & -\tilde{N}\Gamma_\Sigma \\ 0 & I-\tilde{M}\Gamma_\Sigma \end{pmatrix}\begin{pmatrix} I \\ K_2 \end{pmatrix}(I-G_2K_2)^{-1}$ for the coprime factor uncertainties with $W_P = 1$, $W_{RM} = 0.0001$ and $W_{RN} = 0.0001$

Figures 8 and 9 present the frequency responses of the I/O maps for the additive uncertainty and the coprime factor uncertainties with different Σ, respectively. The frequency

responses reveal the robustness of the compensators. Figures 8 and 9 show that the robustness of the antiwindup compensator proposed in this paper is better than that proposed in [22] for the additive uncertainty and the coprime factor uncertainties. The induced L_2-norms of the I/O maps illustrated in Table 3 elucidate the assessments of the robustness between these two antiwindup compensators for the additive uncertainty and the coprime factor uncertainties. The differences in induced L_2-norms for the I/O maps between these two antiwindup compensators become more obvious as the nonlinearity increases, i.e., Σ increases.

TABLE 3. The induced L_2-norms of I/O maps with different Σ in Example 6.3

Σ	$0.3I$	$0.6I$	$0.9I$
$\left\|(I-\tilde{M}\Gamma_\Sigma)K_2(I-G_2K_2)^{-1}\right\|_{i,2}$	94.4983	53.9990	13.4998
$\left\|(I-\bar{\tilde{M}}\Gamma_\Sigma)K_2(I-G_2K_2)^{-1}\right\|_{i,2}$	134.4149	133.6900	129.4575
$\left\|(I-\bar{\tilde{M}}\Gamma_\Sigma)K_2(I-G_2K_2)^{-1}\right\|_{i,2}-\left\|(I-\tilde{M}\Gamma_\Sigma)K_2(I-G_2K_2)^{-1}\right\|_{i,2}$	39.9166	79.6910	115.9578
$\left\|\begin{pmatrix} I & -\tilde{N}\Gamma_\Sigma \\ 0 & I-\tilde{M}\Gamma_\Sigma \end{pmatrix}\begin{pmatrix} I \\ K_2 \end{pmatrix}(I-G_2K_2)^{-1}\right\|_{i,2}$	94.5036	54.0083	13.5367
$\left\|\begin{pmatrix} I & -\bar{\tilde{N}}\Gamma_\Sigma \\ 0 & I-\bar{\tilde{M}}\Gamma_\Sigma \end{pmatrix}\begin{pmatrix} I \\ K_2 \end{pmatrix}(I-G_2K_2)^{-1}\right\|_{i,2}$	134.4186	133.6938	129.4615
$\left\|\begin{pmatrix} I & -\bar{\tilde{N}}\Gamma_\Sigma \\ 0 & I-\bar{\tilde{M}}\Gamma_\Sigma \end{pmatrix}\begin{pmatrix} I \\ K_2 \end{pmatrix}(I-G_2K_2)^{-1}\right\|_{i,2}$ $-\left\|\begin{pmatrix} I & -\tilde{N}\Gamma_\Sigma \\ 0 & I-\tilde{M}\Gamma_\Sigma \end{pmatrix}\begin{pmatrix} I \\ K_2 \end{pmatrix}(I-G_2K_2)^{-1}\right\|_{i,2}$	39.9151	79.6855	115.9248

Figure 10 presents the output time responses of the nominal plant and the perturbed plants. The control input is also assumed to be saturated at ± 1. The reference input pattern is the same as in [22]. These two antiwindup compensators have the same time responses for the nominal plant as shown in Figure 10(a). Figure 10(b) shows the time responses of the compensated system for G_{2P1} with these two compensators. The stable responses reveal that these two compensators are robust enough to stabilize G_{2P1} although oscillation arises more with the compensator in [22] than with the compensator synthesized in this paper. Figures 10(c) and 10(d) compare the time responses of the other two unstable perturbed plants, G_{2P2} and G_{2P3}, respectively. The antiwindup compensator in [22] is also robust for the unstable perturbed plant G_{2P2} but it causes the more oscillatory response compared with that of G_{2P1}. This indicates the compensator in [22] is poor robust for G_{2P2}. As shown in Figure 9(d), the compensator in [22] cannot stabilize G_{2P3} which has an unstable pole farther from image axis than the poles of G_{2P2}. The compensator synthesized in this paper is intuitively superior to that in [22] for both G_{2P2} and G_{2P3}. This compensator is capable of stabilizing not only G_{2P1} and G_{2P2} but G_{2P3}. Furthermore, the responses using the antiwindup compensator synthesized in this paper are less oscillatory. The stable responses imply the proposed approach in this paper has the intrinsic robustness properties when the perturbed plants have different pole numbers on RHP within uncertainties from the nominal plant.

Example 6.4. *A linear rotorcraft model of the Sikorsky S-61 helicopter in hover flight condition with the rotor disk tilted instantaneously is as follows [28].*

$$\dot{x} = Ax + Bu_c,$$
$$y = Cx + Du_c,$$

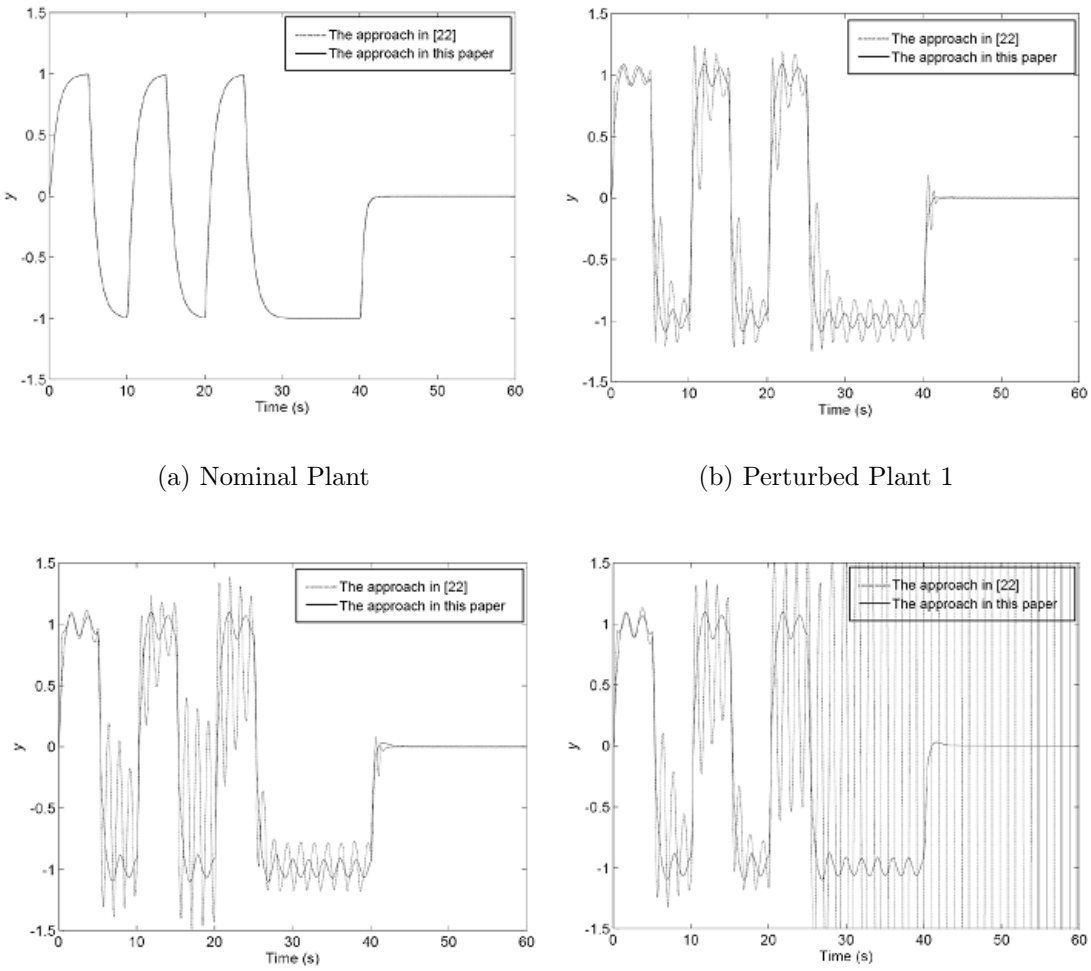

(a) Nominal Plant

(b) Perturbed Plant 1

(c) Perturbed Plant 2

(d) Perturbed Plant 3

FIGURE 10. Output time responses of plants with $W_P = 1$, $W_{RM} = 0.0001$ and $W_{RN} = 0.0001$

where u_c is the control vector, x is the state vector, and y is the measured output vector. u_c, x and y are defined as

$$u_c \equiv \begin{pmatrix} -\phi_R \\ \theta_R \end{pmatrix},$$
$$x \equiv \begin{pmatrix} \theta_F & \phi_F & q_F & p_F & u & v \end{pmatrix}^T$$

and

$$y \equiv \begin{pmatrix} q_F & p_F & -\phi_R & \theta_R \end{pmatrix}^T.$$

θ_F is the pitch attitude of fuselage; ϕ_F is the roll angle of fuselage; q_F is the pitch rate of fuselage; p_F is the roll rate of fuselage; u and v are the velocities along the x-axis and y-axis of the fuselage, respectively; θ_R is the pitch (longitudinal) tilt angle of the rotor; and ϕ_R is the roll (lateral) tilt angle of the rotor. Both θ_R and ϕ_R are assumed to be saturated at 2 units. G_2 which is the nominal transfer function from u_c to y has state

space representation as

$$G_2 \stackrel{S}{=} \left[\begin{array}{cccccc|cc} 0 & 0 & 1 & 0 & 0 & 0 & 0 & 0 \\ 0 & 0 & 0 & 1 & 0 & 0 & 0 & 0 \\ 0 & 0 & -0.042 & 0.32 & 0.003 & 0.001 & -0.3 & 6.3 \\ 0 & 0 & -1.23 & -1.6 & 0.004 & -0.012 & -23 & -1.1 \\ -32.2 & 0 & 4.7 & -1 & -0.02 & -0.005 & 1 & -32.2 \\ 0 & 32.2 & -1 & -4.7 & 0.005 & -0.02 & -32.2 & 1 \\ \hline 0 & 0 & 1 & 0 & 0 & 0 & 0 & 0 \\ 0 & 0 & 0 & 1 & 0 & 0 & 0 & 0 \\ 0 & 0 & 0 & 0 & 0 & 0 & 1 & 0 \\ 0 & 0 & 0 & 0 & 0 & 0 & 0 & 1 \end{array}\right].$$

The eigenvalues of G_2 are -1.4924, -0.6390, $0.0585 \pm 0.5049i$ and $0.1662 \pm 0.3751i$. This helicopter has 4 modes involving 2 stable subsidence (overdamped) modes and 2 unstable oscillation modes (4 eigenvalues on RHP) for the nominal model. The states of this helicopter will diverge due to a small disturbance even the states are all in equilibrium simultaneously. One of the feedback compensator, K_2, synthesized to stabilize G_2 has a state space representation as follows (Refer to Theorem 1 in [25] with $\gamma = 2.7397$ to obtain K_2).

$$K_2 \stackrel{S}{=} \left[\begin{array}{cccccc|cccc} 0 & 0 & 0.9667 & 0.2559 & 0 & 0 & 0.0333 & -0.2559 & 0 & 0 \\ 0 & 0 & -0.2559 & 0.9667 & 0 & 0 & 0.2559 & 0.0333 & 0 & 0 \\ -5.7322 & -0.2912 & -11.4193 & 0.3932 & 0.0224 & -0.0012 & 4.6085 & -0.0364 & 0 & 0 \\ 7.3391 & -10.1627 & -0.9263 & -36.6256 & -0.0329 & -0.0384 & -0.0364 & 14.9563 & 0 & 0 \\ -2.7553 & 1.2519 & -228.8171 & -69.6919 & -0.1198 & 0.0056 & 268.0919 & 68.0397 & 0 & 0 \\ 7.9304 & 17.9085 & -79.0435 & 209.5562 & -0.0387 & -0.0577 & 75.6935 & -242.2332 & 0 & 0 \\ \hline -0.5499 & 0.8861 & 0.0793 & 1.7406 & 0.0029 & 0.0023 & 0 & 0 & -1 & 0 \\ -1.8459 & -0.0502 & -2.145 & 0.0946 & 0.0063 & -0.0006 & 0 & 0 & 0 & -1 \end{array}\right].$$

From Theorem 5.1 with $W_P = 1$, $W_{RM} = 1$ and $W_{RN} = 1$, we have

$$F = \begin{bmatrix} 1.8773 \times 10^{-2} & 1.4766 \times 10^{-1} & 3.6554 \times 10^{-2} & 6.4866 \times 10^{-1} & 1.2102 \times 10^{-4} & 1.2797 \times 10^{-5} \\ -1.5025 \times 10^{-1} & 1.5633 \times 10^{-2} & -7.3015 \times 10^{-1} & 3.0896 \times 10^{-2} & 1.1603 \times 10^{-5} & -1.3782 \times 10^{-4} \end{bmatrix},$$

or the state space representation of the antiwindup compensator is

$$\begin{pmatrix} \tilde{M} - I \\ \tilde{N} \end{pmatrix} \stackrel{S}{=}$$

$$\left[\begin{array}{cccccc|cc} 0 & 0 & 1 & 0 & 0 & 0 & 0 & 0 \\ 0 & 0 & 0 & 1 & 0 & 0 & 0 & 0 \\ -9.5218 \times 10^{-1} & 5.4193 \times 10^{-2} & -4.6529 & 3.2005 \times 10^{-1} & 3.0368 \times 10^{-3} & 1.2790 \times 10^{-4} & -0.3 & 6.3 \\ -2.6652 \times 10^{-1} & -3.4133 & -1.2676 & -16.5531 & 1.2037 \times 10^{-3} & -1.2143 \times 10^{-2} & -23 & -1.1 \\ -27.3433 & -3.5573 \times 10^{-1} & 28.2473 & -1.3462 & -2.0253 \times 10^{-2} & -5.4944 \times 10^{-4} & 1 & -32 \\ -7.5475 \times 10^{-1} & 27.4611 & -2.9072 & -25.5559 & 1.1147 \times 10^{-3} & -2.0550 \times 10^{-2} & -32 & 1 \\ \hline 1.8773 \times 10^{-2} & 1.4766 \times 10^{-1} & 3.6554 \times 10^{-2} & 6.4866 \times 10^{-1} & 1.2102 \times 10^{-4} & 1.2797 \times 10^{-5} & 0 & 0 \\ -1.5025 \times 10^{-1} & 1.5633 \times 10^{-2} & -7.3015 \times 10^{-1} & 3.0896 \times 10^{-2} & 1.1603 \times 10^{-5} & -1.3782 \times 10^{-4} & 0 & 0 \\ \cdots & \cdots & \cdots & \cdots & \cdots & \cdots & \cdots & \cdots \\ 0 & 0 & 1 & 0 & 0 & 0 & 0 & 0 \\ 0 & 0 & 0 & 1 & 0 & 0 & 0 & 0 \\ 1.8773 \times 10^{-2} & 1.4766 \times 10^{-1} & 3.6554 \times 10^{-2} & 6.4866 \times 10^{-1} & 1.2102 \times 10^{-4} & 1.2797 \times 10^{-5} & 1 & 0 \\ -1.5025 \times 10^{-1} & 1.5633 \times 10^{-2} & -7.3015 \times 10^{-1} & 3.0896 \times 10^{-2} & 1.1603 \times 10^{-5} & -1.3782 \times 10^{-4} & 0 & 1 \end{array}\right].$$

Figure 11 sketches the maximal singular values of $(I - \tilde{M}\Gamma_\Sigma)K_2(I - G_2K_2)^{-1}$ with $\Sigma = 0.3I$, $0.6I$ and $0.9I$. That is, the robust bounds for additive uncertainty are 1.0640, 0.7424 and 0.5382 for $\Sigma = 0.3I$, $0.6I$ and $0.9I$, respectively. They reflect the robustness of the antiwindup compensator with different Σ for the additive uncertainty criterion. Similarly, Figure 12 shows the robustness of the same antiwindup compensator for criterion of the coprime factor uncertainties with different Σ. Their robust bounds for coprime factor uncertainties are 0.3995, 0.3223 and 0.1543 for $\Sigma = 0.3I$, $0.6I$ and $0.9I$, respectively.

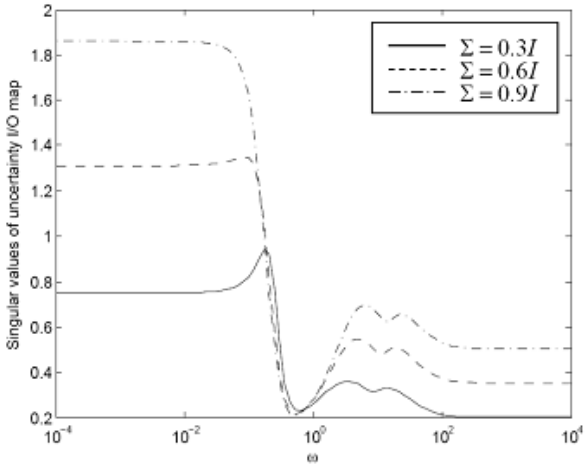

FIGURE 11. The maximal singular values of $(I-\tilde{M}\Gamma_\Sigma)K_2(I-G_2K_2)^{-1}$ for the robustness of the additive uncertainty criterion

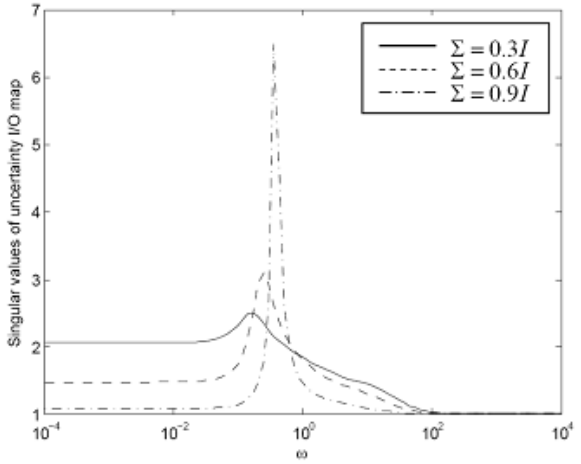

FIGURE 12. The maximal singular values of $\begin{pmatrix} I & -\tilde{N}\Gamma_\Sigma \\ 0 & I-\tilde{M}\Gamma_\Sigma \end{pmatrix}\begin{pmatrix} I \\ K_2 \end{pmatrix}(I-G_2K_2)^{-1}$ for the robustness of the criterion of coprime factor uncertainties

Let G_{2P} be a perturbed plant of G_2 and

$$G_{2P} \stackrel{S}{=} \left[\begin{array}{cccccc|cc} 0 & 0 & 1 & 0 & 0 & 0 & 0 & 0 \\ 0 & 0 & 0 & 1 & 0 & 0 & 0 & 0 \\ 0 & 0 & -0.042 & 0.32 & 0.003 & 0.001 & -0.3 & 6.3 \\ 0 & 0 & -2.5 & -1.6 & 0.004 & -0.012 & -23 & -1.1 \\ -32.2 & 0 & 2.5 & -1 & -0.02 & -0.005 & 1 & -32.2 \\ 0 & 32.2 & -1 & -4.7 & 0.005 & -0.02 & -32.2 & 1 \\ \hline 0 & 0 & 1 & 0 & 0 & 0 & 0 & 0 \\ 0 & 0 & 0 & 1 & 0 & 0 & 0 & 0 \\ 0 & 0 & 0 & 0 & 0 & 0 & 1 & 0 \\ 0 & 0 & 0 & 0 & 0 & 0 & 0 & 1 \end{array}\right].$$

The eigenvalues of G_{2P} are $-0.9828 \pm 0.1855i$, $0.0078 \pm 0.5442i$ and $0.1496 \pm 0.3429i$. There are 2 poles on RHP which is different from those of G_2. Figures 13 and 14 show the time responses of θ_F, ϕ_F, $-\phi_R$ and θ_R with initial conditions for G_2 and G_{2P}, respectively.

They reveal that the antiwindup compensator is robust not only for G_2 but also for G_{2P} although the numbers of poles on RHP are different between G_2 and G_{2P}.

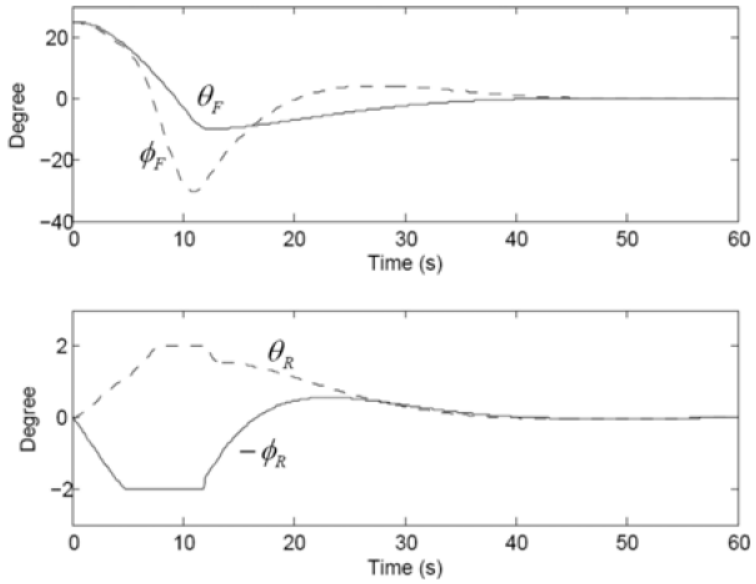

FIGURE 13. Time responses of states and inputs for the G_2

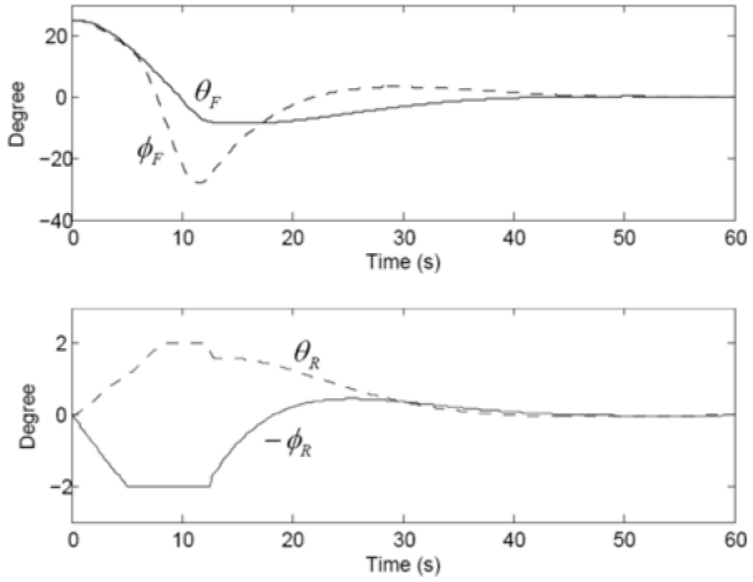

FIGURE 14. Time responses of states and inputs for the G_{2P}

7. **Conclusions.** This study presented a robust antiwindup synthesis for a plant subject to input saturation and coprime factor uncertainties. Input saturation deteriorates the robustness of the compensated systems. $\left\| \begin{pmatrix} I & -\tilde{N}\Gamma_\Sigma \\ 0 & I - \tilde{M}\Gamma_\Sigma \end{pmatrix} \right\|_{i,2}$ is the input saturation penalty for a plant subject to coprime factor uncertainties. In case of the robustness criterion of a compensator for a plant subject to additive uncertainties, the penalty becomes $\left\| (I - \tilde{M}\Gamma_\Sigma) \right\|_{i,2}$. This study also proposed a more general framework to treat plants subject to both coprime factor and additive uncertainties. The criteria listed in Table 1 can

evaluate the robustness for the additive uncertainty or for the coprime factor uncertainties with or without input saturation. The framework approach in this paper can be an alternative application in arduous situations such as uncertain plants with different pole numbers on RHP. The antiwindup compensator can be also synthesized based on the LMI technique for the robustness requirements as well as the optimization for robustness and performance of a compensated system subject to both input saturation and coprime factor uncertainties.

Example 6.3 presented that the robustness and performance of the antiwindup compensator synthesized in this paper are superior to those in [22] for both the additive uncertainty and the coprime factor uncertainties. According to the result in Example 6.1, the robustness of the antiwindup compensator using the approach presented in this paper is not always preferable to those by other approaches when other robustness criteria are applied. However, the proposed antiwindup compensator synthesized in this paper is more applicable than others if the robustness measurement is evaluated by the coprime factor uncertainties. That is, this proposed approach is more robust when the uncertain plant has different pole numbers on RHP within uncertainties. A practical example was illustrated in Example 6.4 to demonstrate the synthesis process. A robust feedback controller is essential in order to provide enough robust bound for the antiwindup compensator since there exists penalty for nonlinearity of input saturation. The results show that the antiwindup compensator is robust against the input saturation nonlinear and the different pole numbers on RHP.

A scheme called weaken antiwindup is expected to improve the robustness to saturated systems after slightly adjusting the linear loop [29]. The output feedback compensators for weakened antiwindup of coprime factor uncertainties will be one of the further researches.

Acknowledgment. This research work is supported by National Science Council under Grand NSC 98-2511-S-018-007 and NSC 100-2623-E-018-003-D.

REFERENCES

[1] R. Hanus, Antiwindup and bumpless transfer: A survey, *Proc. of the 12th IMACS World Congress*, Paris, France, pp.59-65, 1988.

[2] M. V. Kothare, P. J. Campo, M. Morari and C. N. Nett, A unified framework for the study of anti-windup designs, *Automatica*, vol.30, pp.1869-1883,1994.

[3] P. Hippe and C. Wurmthaler, Systematic closed-loop design in the presence of input saturation, *Automatica*, vol.35, pp.689-695, 1999.

[4] P. J. Campo, M. Morari and N. C. Nett, Multivariable antiwindup and bumpless transfer: A general theory, *Proc. of American Control Conference*, Pittsburgh, U.S.A., 1989.

[5] C. Edwards and I. Postlethwaite, An anti-windup scheme with closed-loop stability considerations, *Automatica*, vol.35, pp.761-765, 1999.

[6] S. Crawshaw and G. Vinnicombe, Anti-windup synthesis for guaranteed l2 performance, *Proc. of American Control Conference*, Anchorage, U.S.A., pp.657-661, 2002.

[7] S. Miyamoto and G. Vinnicombe, Robust control of plants with saturation nonlinearity based on coprime factor representation, *Proc. of the 36th IEEE Conference on Decision & Control*, Kobe, Japan, pp.2838-2840, 1996.

[8] J. S. Shamma, Anti-windup via constrained regulation with observers, *Systems & Control Letters*, vol.40, pp.261-268, 2000.

[9] D. Angeli and E. Mosca, Command governors for constrained nonlinear systems, *IEEE Transactions on Automatic Control*, vol.44, pp.816-820, 1999.

[10] E. Gilbert and I. Kolmanovsky, Fast reference governors for systems with state and control constraints and disturbance inputs, *International Journal of Robust and Nonlinear Control*, vol.9, pp.1117-1141, 1999.

[11] F. Wu, Z. Li and Q. Zheng, Output feedback stabilization of linear systems with actuator saturation, *IEEE Transactions on Automatic Control*, vol.52, pp.122-128, 2007.

[12] T. Hu, A. R. Teel and L. Zaccarian, Anti-windup synthesis for linear control systems with input saturation: Achieving regional, nonlinear performance, *Automatica*, vol.44, pp.512-519, 2008.
[13] G. Herrmann, B. Hredzak, M. C. Turner, I. Postlethwaite and G. Guo, Discrete robust anti-windup to Improve a novel dual-stage large-span track-seek/following method, *IEEE Transactions on Control Systems Technology*, vol.16, pp.1342-1351, 2008.
[14] M. Turner and L. Zaccarian, Special issue: Anti-windup, *International Journal of Systems Science*, vol.37, pp.65-139, 2006.
[15] L.-Y. Sun, J. Zhao and G. M. Dimirovski, Nonlinear robust controller design for thyristor controlled series compensation, *International Journal of Innovative Computing, Information and Control*, vol.5, no.4, pp.981-989, 2009.
[16] H. Han, Adaptive fuzzy control for a class uncertain nonlinear systems via LMI approach, *International Journal of Innovative Computing, Information and Control*, vol.6, no.1, pp.275-285, 2010.
[17] J.-D. Hwang and Z.-R. Tsai, Robust self-tuning fuzzy tracker design of time-varying nonlinear systems via conditional-LMI approach, *International Journal of Innovative Computing, Information and Control*, vol.6, no.6, pp.2621-2636, 2010.
[18] J. Manoel, Jr. Gomes da Silva and S. Tarbouriech, Anti-windup design with guaranteed regions of stability: An LMI-based approach, *IEEE Transactions on Automatic Control*, vol.50, pp.106-111, 2005.
[19] S. Galeani, S. Onori, A. R. Teel and L. Zaccarian, A magnitude and rate saturation model and its use in the solution of a static anti-windup problem, *Systems & Control Letters*, vol.57, pp.1-9, 2008.
[20] S. Tarbouriech and G. Garcia, *Control of Uncertain Systems with Bounded Inputs*, Springer-Verlag, London, 1997.
[21] M. C. Turner, G. Herrmann and I. Postlethwaite, Accounting for the uncertainty in anti-windup synthesis, *Proc. of American Control Conference*, Boston, U.S.A., pp.5292-5297, 2004.
[22] M. C. Turner, G. Herrmann and I. Postlethwaite, Incorporating robustness requirements into anti-windup design, *IEEE Transactions on Automatic Control*, vol.52, pp.1842-1855, 2007.
[23] K. Glover and D. McFarlane, Robust stabilization of normalized coprime factor plant descriptions with bounded uncertainty, *IEEE Transactions on Automatic Control*, vol.34, pp.821-830, 1989.
[24] M. Deng, N. Bu and A. Inoue, Output tracking of nonlinear feedback systems with perturbation based on robust right coprime factorization, *International Journal of Innovative Computing, Information and Control*, vol.5, no.10(B), pp.3359-3366, 2009.
[25] J. S. Young, Synthesis of decoupling controller for non-minimum phase plants of different pole numbers on RHP within uncertainties, *International Journal of Systems Science*, vol.42, pp.939-950, 2011.
[26] P. Weston and I. Postlethwaite, Linear conditioning for systems containing saturating actuators, *Automatica*, vol.36, pp.1347-1354, 2000.
[27] S. Skogestad and I. Postlethwaite, *Multivariable Feedback Control: Analysis and Design*, 2nd Edition, Wiley, UK, 2005.
[28] D. McLean, *Automatic Flight Control Systems*, Prentice Hall, New York, 1990.
[29] S. Galeani, S. Nicosa, A. Teel and L. Zaccarian, Output feedback compensators for weakened anti-windup of additively perturbed systems, *Proc. of IFAC World Congress*, 2005.